Hidden quantum Hall stripes in $Al_xGa_{1-x}As/Al_{0.24}Ga_{0.76}As$ quantum wells

X. Fu,[1] Y. Huang,[1] B. I. Shklovskii,[1] M. A. Zudov,[1,*] G. C. Gardner,[2,3] and M. J. Manfra[2,3,4,5]

[1] *School of Physics and Astronomy, University of Minnesota, Minneapolis, Minnesota 55455, USA*
[2] *Microsoft Quantum Lab Purdue, Purdue University, West Lafayette, Indiana 47907, USA*
[3] *Birck Nanotechnology Center, Purdue University, West Lafayette, Indiana 47907, USA*
[4] *Department of Physics and Astronomy, Purdue University, West Lafayette, Indiana 47907, USA*
[5] *School of Electrical and Computer Engineering and School of Materials Engineering, Purdue University, West Lafayette, Indiana 47907, USA*

(Received October 11, 2020)

We report on transport signatures of hidden quantum Hall stripe (hQHS) phases in high ($N > 2$) half-filled Landau levels of $Al_xGa_{1-x}As/Al_{0.24}Ga_{0.76}As$ quantum wells with varying Al mole fraction $x < 10^{-3}$. Residing between the conventional stripe phases (lower N) and the isotropic liquid phases (higher N), where resistivity decreases as $1/N$, these hQHS phases exhibit isotropic and N-independent resistivity. Using the experimental phase diagram we establish that the stripe phases are more robust than theoretically predicted, calling for improved theoretical treatment. We also show that, unlike conventional stripe phases, the hQHS phases do not occur in ultrahigh mobility GaAs quantum wells, but are likely to be found in other systems.

Discovery of the integer quantum Hall effect in Si [1] has paved the way to observations of many exotic phenomena in two-dimensional (2D) electron and hole systems. Two prime examples are the fractional quantum Hall effect [2] and the quantum Hall stripes (QHSs) [3–7]. While fractional quantum Hall effects have been realized in many systems, including GaAs [2], Si [8, 9], AlAs [10], GaN [11], graphene [12, 13], CdTe [14], ZnO [15], Ge [16], and InAs [17], exploration of the QHS physics remains limited to GaAs [18].

Forming due to a peculiar box-like screened Coulomb potential, QHSs can be viewed as charge density waves consisting of stripes with alternating integer filling factors ν, e.g., $\nu = 4$ and $\nu = 5$ [19]. In experiments, QHSs are manifested by giant resistivity anisotropies ($\rho_{xx} \gg \rho_{yy}$) in $N \geq 2$ half-filled Landau levels (LLs). Appearance of these anisotropies in macroscopic samples is attributed to a misterious symmetry breaking field [20–23] which nearly always aligns QHSs along $\hat{y} \equiv \langle 110 \rangle$ crystal axis of GaAs [24]. While a sufficiently low disorder is necessary for the QHS formation, the absence of QHSs in systems beyond GaAs might simply be due to the lack of symmetry-breaking fields [25]. Indeed, electron bubble phases [3–5, 26–35], which are close relatives of QHSs, have already been identified in graphene [36].

In this Letter we report observation of the recently predicted [37] hidden QHS (hQHS) phases in a series of $Al_xGa_{1-x}As/Al_{0.24}Ga_{0.76}As$ quantum wells with $x < 10^{-3}$. In contrast to the ordinary QHS phases, the hQHS phases are characterized by isotropic resistivity ($\rho_{xx} = \rho_{yy} = \rho$) which is independent of ν, unlike the isotropic liquid phases in which $\rho \propto \nu^{-1}$. These unique properties make these phases detectable without symmetry-breaking fields thereby opening an avenue to study stripe physics in systems beyond GaAs. The wide variation of mobilities in our samples allows us to construct an experimental phase diagram in the conductivity-filling factor plane. Its comparison to theoretical predictions [37] yields the electron quantum lifetimes and the stripe density of states. The latter turns out to be lower than predicted by original Hartree-Fock theory [3, 4], calling for further theoretical input. We confirm this finding by a complementary experiment on an ultrahigh mobility GaAs quantum well, where we also show that in this sample the hQHS phase yields to the QHS phase, in agreement with the theory.

Before presenting our experimental data, we briefly summarize the physics behind the hQHS phases [37]. The resistance anisotropies in the ordinary QHS phase emerge due to different diffusion mechanisms along and perpendicular to the stripes [38, 39]. In this picture, an electron drifts a distance L_y along the y-oriented stripe edge in an x-directed internal electric field until it is scattered by impurities to one of the adjacent stripe edges located at a distance $L_x = \Lambda/2 \approx \sqrt{2}R_c$ [3, 4], where Λ is the stripe period and R_c is the cyclotron radius. When $L_y \gg L_x$, the diffusion coefficient in the $\hat{y}$ direction is much larger that in the $\hat{x}$ direction which leads to anisotropic conductivity, $\sigma_{yy} \gg \sigma_{xx}$, and resistivity, $\rho_{xx} \gg \rho_{yy}$. Since $L_y \propto \nu^{-1}$ and $L_x \propto \nu$ [39], the anisotropy decreases with ν and eventually vanishes at some $\nu = \nu_1$. At larger ν, the drift contribution to the diffusion along stripes can be neglected and L_y, like L_x, is determined entirely by the impurity scattering. For isotropic scattering, it is easy to show [40] that $L_y = \sqrt{2}R_c$ which coincides with L_x. As a result, the QHS phase yields to the hQHS phase in which the resistivity is isotropic and ν-independent (since the stripe density of states does not vary with ν). The hQHS phase persists till the stripe structure is destroyed by disorder at $\nu = \nu_2$ and the ground state becomes an isotropic liquid with $\rho_{xx} = \rho_{yy} \propto \nu^{-1}$, as predicted by Ando and Uemura [41] and experimentally confirmed by Coleridge, Zawadski, and Sachrajda (CZS) [42].

For the hQHS phase to exist and be detected, it should span a sizable range of the filling factors, $\Delta\nu = \nu_2 - \max\{\nu_1, 9/2\} \gg 1$. The range $\Delta\nu$ depends sensitively on both transport τ^{-1} and quantum τ_q^{-1} scattering rates, which control ν_1 and ν_2, respectively [37]. As we will see, ultrahigh mobility GaAs quantum wells do not support the hQHS phase as $\nu_1 \approx \nu_2$ in these samples. On the other hand, adding the correct small amount of Al [43] to the GaAs well greatly expands $\Delta\nu$, as it affects ν_1 to a much greater extent than it does ν_2. This happens because Al acts as a short-range disorder, which contributes *equally* to transport τ^{-1} and quantum $\tau_{\rm q}^{-1}$ scattering rates, and because $\tau_{\rm q}/\tau \ll 1$ at $x = 0$.

Apart from different x, all our $\mathrm{Al}_x\mathrm{Ga}_{1-x}\mathrm{As}$ quantum wells share identical heterostructure design [44]. Electrons are supplied by Si doping in narrow GaAs wells surrounded by narrow AlAs layers and placed at a setback distance of 75 mm from each side of the 30-mm-wide $\mathrm{Al}_x\mathrm{Ga}_{1-x}\mathrm{As}$ well hosting the 2D electrons. Parameters of samples A, B, and C, such as Al mole fraction x, electron density n_e, mobility μ, and Drude conductivity $\tilde{\sigma}_0 = h n_e \mu / e$ in units of e^2/h at zero magnetic field ($B = 0$) are listed in Table I. The samples are approximately 4 mm squares with eight indium contacts positioned at the corners and at the midsides. Longitudinal resistances R_{xx} and R_{yy} were measured in sweeping magnetic fields using a four-terminal, low-frequency (a few Hz) lock-in technique at a temperature $T \approx 25$ mK. The current was sent along either $\hat{x} \equiv \langle 1\bar{1}0\rangle$ or $\hat{y} \equiv \langle 110\rangle$ direction using the midside contacts and the voltage was measured between contacts along the edge. To account for anisotropies due to non-ideal geometry, R_{xx} or R_{yy} was multiplied by a factor (typically $\lesssim 1.1$) which was chosen to make $R_{xx} = R_{yy}$ in the low field regime.

In Fig. 1 we present longitudinal resistances R_{xx} and R_{yy} as a function of filling factor ν measured in sample B. At low half-integer filling factors, such as $\nu = 9/2$, $11/2$ and $13/2$, the data reveal conventional QHS phases, as evidenced by $R_{xx} > R_{yy}$. At high half-integer filling factors, such as $\nu > 25/2$, we identify the CZS phase in which $R_{xx} \approx R_{yy} \propto \nu^{-1}$ (cf. dash-dotted line). At intermediate half-integer filling factors, $\nu = 15/2, ..., 23/2$, one readily confirms *both* characteristic features of the hQHS phase; indeed, the data show that two longitudinal resistances are practically the same ($R_{xx} \approx R_{yy}$) and are *independent* of ν (cf. dashed line). From Fig. 1, we can easily identify the characteristic filling factors $\nu_1 \approx 7$ and $\nu_2 \approx 12.5$ which mark the crossovers from the QHS to the hQHS phase and from the hQHS to the CZS phase, respectively.

In a similar manner, we have obtained ν_1 and ν_2 for sample A and ν_2 for sample C (which does not support the QHS phase due to higher Al mole fraction x), which we then use to construct the experimental phase diagram shown in Fig. 2. We start by adding points representing the dimensionless Drude conductivity $\tilde{\sigma}_0$ for samples A, B, C, see Table I, and corresponding filling factors ν_1 (solid circles) and ν_2 (solid squares) To connect these data points we use the

TABLE I. Sample ID, Al mole fraction x, electron density n_e, mobility μ, and Drude conductivity, in units of e^2/h, $\tilde{\sigma}_0 = h n_e \mu / e$ at zero magnetic field ($B = 0$).

Sample ID	x	n_e (10^{11} cm^{-2})	μ (10^6 cm^2/Vs)	$\tilde{\sigma}_0$ (10^3)
A	0.00057	3.0	6.5	8.0
B	0.00082	2.9	4.1	4.9
C	0.0078	2.7	1.2	1.3

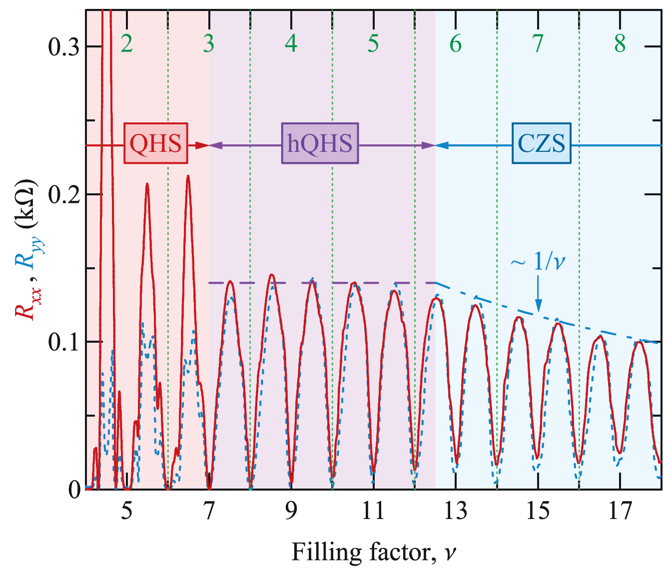

FIG. 1. Longitudinal resistances R_{xx} (solid line) and R_{yy} (dotted line) as a function of the filling factor ν measured in sample B. Gap centers between spin-resolved Landau levels are labeled by $N = 2, 3, , ..$ at the top axis ($\nu = 2N + 1$). The conventional QHS phase ($R_{xx} > R_{yy}$) and the CZS phase ($R_{xx} \approx R_{yy} \propto \nu^{-1}$) occur at half-integer $\nu = 9/2, 11/2, 13/2$ and at $\nu = 27/2, 29/2, ...$, respectively. The hQHS phase is identified at intermediate half-integer filling factors, $\nu = 15/2, ..., 25/2$, where the resistance is isotropic *and* $\nu-$ independent. The characteristic ν^0 (ν^{-1}) dependence of the isotropic resistance in the hQHS (CZS) phase is marked by dashed (dash-dotted) line.

theoretical boundaries of the hQHS phase [37]. The lower boundary, $\nu = \nu_1$, separating the QHS and the hQHS phases, is given by [37]

$$\nu_1 \simeq \frac{\sqrt{\tilde{\sigma}_0}}{\alpha}\,, \tag{1}$$

where α [45] is the QHS density of states in units of the density of states per spin at $B = 0$, $g_0 = m^\star/2\pi\hbar^2$. This boundary can be obtained by either matching the parameter-free geometric average of the resistivities in the QHS phase $\sqrt{\rho_{xx}\rho_{yy}} = (h/e^2)/(2\nu^2 + 1/2) \approx (h/e^2)/2\nu^2$ [38, 39] and the resistivity in the hQHS phase [37],

$$\tilde{\rho}_{\rm hQHS} \equiv \frac{h}{e^2}\frac{\alpha^2}{2\tilde{\sigma}_0}\,, \tag{2}$$

or, equivalently, by setting the resistivity anisotropy ratio to unity, $\rho_{xx}/\rho_{yy} \approx (\tilde{\sigma}_0/\alpha^2\nu^2)^2 = 1$ [37, 39].

The higher boundary, $\nu = \nu_2$, marks the crossover from the hQHS to the CZS phase and is represented by

$$\nu_2 \simeq \frac{\tilde{\sigma}_0}{\alpha^2}\frac{\tau_{\rm q}}{\tau}\,. \tag{3}$$

This boundary can be obtained by equating α and the density of states at the center of the Landau level in CZS phase, in units of the density of states at $B = 0$, $\sqrt{\omega_{\rm c}\tau_{\rm q}}$ [47, 48] or by

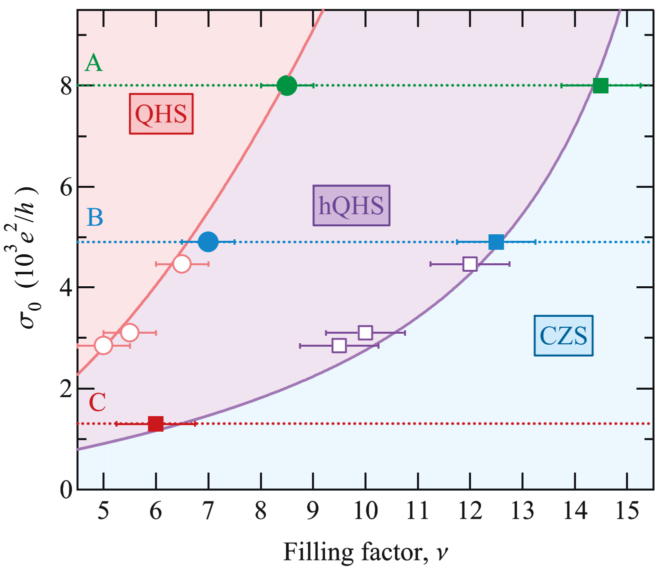

FIG. 2. A diagram in the (ν, σ_0)-plane showing QHS, hQHS, and CZS phases. Solid lines represent crossovers between phases, Eq. (1) (left/upper line) and Eq. (3) (right/lower line). Solid circles (solid squares) represent experimental ν_1 (ν_2) and horizontal dotted lines mark $\tilde{\sigma}_0$ for samples A-C [44]. Open circles (squares) are additional data from a study conducted in a different context which conform to our present findings [46].

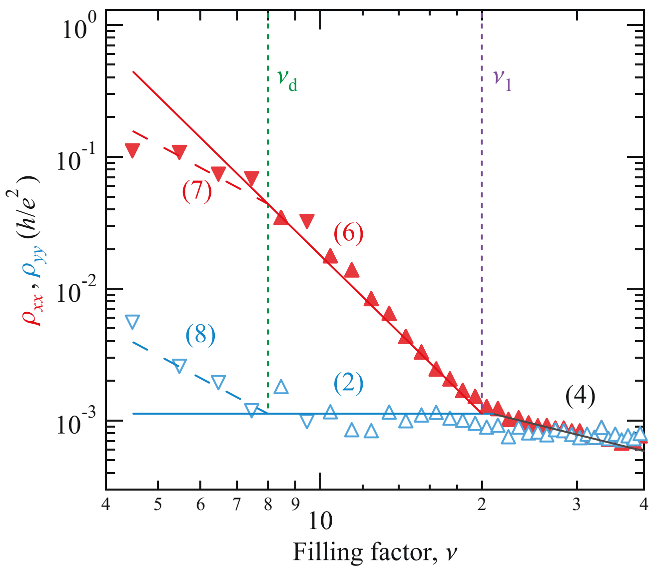

FIG. 3. ρ_{xx} (solid triangles) and ρ_{yy} (open triangles) [63]) as a function of filling factor ν for sample A of Ref. 39 measured at $T \approx 50$ mK. Lines are computed using theoretical expressions, marked by equation numbers.

matching $\rho_{\rm hQHS}$ and the resistivity in the CZS phase [42],

$$\rho_{\rm CZS} \equiv \frac{h}{e^2}\frac{1}{\nu}\frac{\tau_{\rm q}/2\tau}{(\tau_{\rm q}/2\tau)^2+1} \approx \frac{h}{e^2}\frac{1}{\nu}\frac{\tau_{\rm q}}{2\tau}\,. \tag{4}$$

We thus see that for a given carrier density, as mentioned above, ν_2 and ν_1 are controlled by τ and $\tau_{\rm q}$, respectively. Strictly speaking, Eqs. (1), (3) are not sharp boundaries but rather gradual crossovers between corresponding phases.

With the help of Eq. (1) and experimental values of ν_1 in samples A and B, we estimate $\alpha \approx 11$, which is smaller than the theoretical estimate of $\alpha \simeq 18$ [39, 45]. We then parametrize scattering rates τ^{-1} and $\tau_{\rm q}^{-1}$ as

$$\tau^{-1} = \tau_0^{-1} + \kappa x\,, \quad \tau_{\rm q}^{-1} = \tau_{\rm q0}^{-1} + \kappa x\,, \tag{5}$$

where x is the Al mole fraction, $\kappa \approx 24$ ns^{-1} per % Al [44], and $\tau_0^{-1} \approx 3$ ns^{-1} [44] is the transport scattering rate in the limit of $x \to 0$. To find the remaining parameter $\tau_{\rm q0}^{-1}$, which is the quantum scattering rate in the limit of $x \to 0$, we use experimental ν_2 values and notice that Eqs. (1), (3) yield $\tau_{\rm q}/\tau \simeq \nu_2/\nu_1^2$. Using Eq. (5) we then obtain an estimate for $\tau_{\rm q0} \simeq 0.05$ ns which is in good agreement with $\tau_{\rm q}$ values found from low B experiments [49–51] on microwave-induced [52–54] and Hall field-induced [55–57] resistance oscillations in GaAs quantum wells.

We next use $n_e = 3 \times 10^{11}$ cm^{-2} and $m^\star = 0.06\,m_0$ [58–62] to compute the phase boundaries, Eqs. (1), (3), which are shown in Fig. 2 by solid lines. Both lines pass in close proximity to the experimentally obtained ν_1 (solid circles) and ν_2 (solid squares) from all samples, showing excellent agreement between theory [37] and experiment. Finally, we add data points (open circles and squares) from three other $\mathrm{Al}_x\mathrm{Ga}_{1-x}\mathrm{As}/\mathrm{Al}_{0.24}\mathrm{Ga}_{0.76}\mathrm{As}$ quantum wells which were investigated in a different context [46]. These points are also in agreement with both the theory and the present experiment.

Having confirmed the existence of the hQHS phases in $\mathrm{Al}_x\mathrm{Ga}_{1-x}\mathrm{As}/\mathrm{Al}_{0.24}\mathrm{Ga}_{0.76}\mathrm{As}$ quantum wells, we next examine the possibility for these phases to exist in ultra-high mobility GaAs quantum wells (without alloy disorder). In such samples, the lower boundary ν_1, Eq. (1), might approach and even merge with the higher boundary ν_2, Eq. (3), eliminating the hQHS phase as a result. To test this prediction, we revisit the data obtained from sample A of Ref. 39 with $\tilde{\sigma}_0 \approx 3.6 \times 10^4$, much higher than in samples used in the present study. As illustrated in Fig. 3, showing ρ_{xx} (solid triangles) and ρ_{yy} (open triangles) [63] as a function of the filling factor ν, the QHSs anisotropy in this sample collapses at $\nu_1 \approx 20$. Using Eq. (1), we can then estimate $\alpha = \sqrt{\tilde{\sigma}_0}/\nu_1 \approx 10$ [64]. With $\tau_{\rm q} \simeq 0.05$ ns, Eq. (3) gives $\nu_2 \approx 21$ which is very close to $\nu_1 \approx 20$. Indeed, the data in Fig. 3 show that the QHS phase crosses over directly to the CZS phase, bypassing the intermediate hQHS phase.

In the QHS phase, the easy resistivity is ν-independent and is described by $\rho_{yy} = \rho_{\rm hQHS}$, Eq. (2), while the hard resisitivty exhibits clear ν^{-4} dependence and follows [37]

$$\rho_{xx} \simeq \frac{h}{e^2}\frac{\tilde{\sigma}_0}{2\alpha^2\nu^4}\,. \tag{6}$$

However, the agreement between theory and experiment breaks down at $\nu < \nu_{\rm d} \approx 8$, where one observes significant deviations leading to the reduction of the anisotropy. While the nature of such reduction is unclear, it increases upon further cooling and might reflect a crossover to another ground

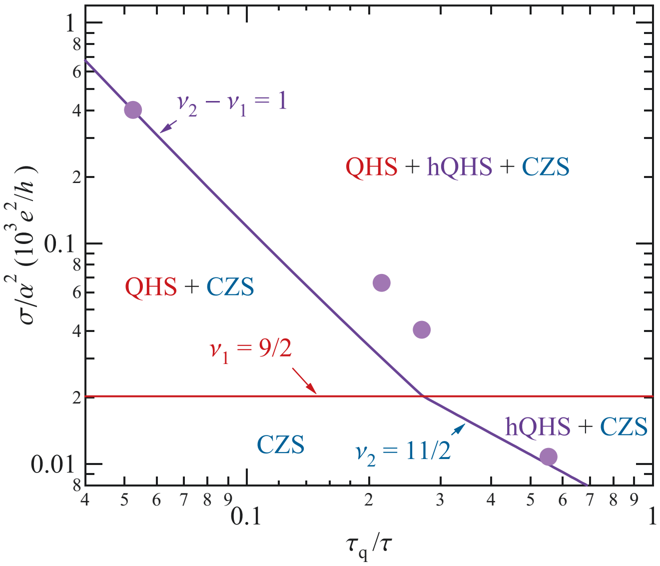

FIG. 4. A diagram in the $(\tau_q/\tau, \sigma_0/\alpha^2)$-plane showing four regions marked by detectable phases. Circles are experimental data points from all four samples studied.

state [65, 66]. We can account for the observed anisotropy reduction at lower filling factors assuming that the QHS phase has a finite concentration of dislocations separated by an average distance $L_d = \beta\Lambda/2$ along stripes, where β is a numerical factor. Scattering of drifting electrons by these dislocations limits their drift length by $L_d \ll L_y$ and the resistivities calculated in Refs. 39, 37 need to be modified to [67, 68]

$$\rho_{xx} = \frac{h}{e^2}\frac{\beta}{2\nu^2}\,, \tag{7}$$

$$\rho_{yy} = \frac{h}{e^2}\frac{1}{2\beta\nu^2}\,. \tag{8}$$

Equations (7), (8) are plotted as dashed lines in Fig. 3. Equating Eq. (7) to Eq. (6) [or Eq. (8) to Eq. (2)], we find that the crossover to the dislocation limited transport happens at

$$\nu_d \equiv \frac{\nu_1}{\sqrt{\beta}}\,. \tag{9}$$

With $\nu_d \simeq 8$ and $\nu_1 \simeq 20$ we find $\beta = (\nu_1/\nu_d)^2 \simeq 6.3$. This value does not seem unreasonable and correctly accounts for the saturation of the anisotropy, $\rho_{xx}/\rho_{yy} = \beta^2 \approx 40$ [39].

Our experimental findings in Al_xGa_{1-x} quantum wells (Fig. 2) and in a clean GaAs quantum well (Fig. 3) can be unified in a phase diagram shown in Fig. 4 which treats σ_0/α^2 and τ_q/τ as independent parameters. Here, the QHS phase is observed above the horizontal line corresponding to $\nu_1 = 9/2$. To detect the hQHS phase, one should satisfy both $\nu_2 - \nu_1 > 1$ and $\nu_2 > 11/2$, since at least two half-integer filling factors are needed to establish ν-independence of the resistance [69]. As a result, the most favorable conditions for the hQHS phase are realized at the top-right corner of the diagram. However, as demonstrated by our experiments on $Al_xGa_{1-x}As$ quantum wells, the hQHS can be detected at modest mobilities provided that the ratio τ_q/τ is sufficiently high. On the other hand, this ratio is much smaller in clean GaAs quantum wells which makes the hQHS detection difficult in such systems despite their high mobility. The phase diagram shown in Fig. 4 provides a a road map for future experiments aiming to detect the hQHS phases.

In summary, we have observed hidden quantum Hall stripe (hQHS) phases [37] forming near half-integer filling factors of $Al_xGa_{1-x}As/Al_{0.24}Ga_{0.76}As$ quantum wells with varying x. These phases reside between the conventional stripe phases and the isotropic liquid phases and are characterized by isotropic resistivity which is not sensitive to the filling factor. Analysis of the experimental phase diagram reveals that the QHS density of states is smaller than predicted by the Hartree-Fock theory [3, 4], calling for improved theory. The unique transport characteristics of the hQHS phases should allow exploration of the stripe physics in 2D systems which, unlike GaAs, lack symmetry breaking fields. On the other hand, ultrahigh mobility GaAs quantum wells favor conventional QHSs over hQHSs due to a shrinking filling factor range where the hQHS phases can form.

We thank G. Jones, T. Murphy, and A. Bangura for technical support. Calculations by Y.H. were supported primarily by the National Science Foundation through the University of Minnesota MRSEC under Award Number No. DMR-1420013 and DMR-2011401. Experiments by X.F. and M.Z. were supported by the U.S. Department of Energy, Office of Science, Basic Energy Sciences, under Award DE-SC0002567. Growth of quantum wells at Purdue University was supported by the U.S. Department of Energy, Office of Science, Basic Energy Sciences, under Award DE-SC0006671. A portion of this work was performed at the National High Magnetic Field Laboratory, which is supported by National Science Foundation Cooperative Agreement Nos. DMR-1157490, DMR-1644779 and the State of Florida.

* Corresponding author: zudov001@umn.edu

[1] K. von Klitzing, G. Dorda, and M. Pepper, *New Method for High-Accuracy Determination of the Fine-Structure Constant Based on Quantized Hall Resistance*, Phys. Rev. Lett. **45**, 494 (1980).

[2] D. C. Tsui, H. L. Stormer, and A. C. Gossard, *Two-Dimensional Magnetotransport in the Extreme Quantum Limit*, Phys. Rev. Lett. **48**, 1559 (1982).

[3] A. A. Koulakov, M. M. Fogler, and B. I. Shklovskii, *Charge density wave in two-dimensional electron liquid in weak magnetic field*, Phys. Rev. Lett. **76**, 499 (1996).

[4] M. M. Fogler, A. A. Koulakov, and B. I. Shklovskii, *Ground state of a two-dimensional electron liquid in a weak magnetic field*, Phys. Rev. B **54**, 1853 (1996).

[5] R. Moessner and J. T. Chalker, *Exact results for interacting electrons in high Landau levels*, Phys. Rev. B **54**, 5006 (1996).

[6] M. P. Lilly, K. B. Cooper, J. P. Eisenstein, L. N. Pfeiffer,

and K. W. West, *Evidence for an Anisotropic State of Two-Dimensional Electrons in High Landau Levels*, Phys. Rev. Lett. **82**, 394 (1999).

[7] R. R. Du, D. C. Tsui, H. L. Stormer, L. N. Pfeiffer, K. W. Baldwin, and K. W. West, *Strongly anisotropic transport in higher two-dimensional Landau levels*, Solid State Commun. **109**, 389 (1999).

[8] S. F. Nelson, K. Ismail, J. J. Nocera, F. F. Fang, E. E. Mendez, J. O. Chu, and B. S. Meyerson, *Observation of the fractional quantum Hall effect in Si/SiGe heterostructures*, Appl. Phys. Lett. **61**, 64 (1992).

[9] T. M. Kott, B. Hu, S. H. Brown, and B. E. Kane, *Valley-degenerate two-dimensional electrons in the lowest Landau level*, Phys. Rev. B **89**, 041107(R) (2014).

[10] E. P. De Poortere, Y. P. Shkolnikov, E. Tutuc, S. J. Papadakis, M. Shayegan, E. Palm, and T. Murphy, *Enhanced electron mobility and high order fractional quantum Hall states in AlAs quantum wells*, Appl. Phys. Lett. **80**, 1583 (2002).

[11] M. J. Manfra, N. G. Weimann, J. W. P. Hsu, L. N. Pfeiffer, K. W. West, S. Syed, H. L. Stormer, W. Pan, D. V. Lang, S. N. G. Chu, et al., *High mobility AlGaN/GaN heterostructures grown by plasma-assisted molecular beam epitaxy on semi-insulating GaN templates prepared by hydride vapor phase epitaxy*, Journal of Applied Physics **92**, 338 (2002), https://doi.org/10.1063/1.1484227.

[12] X. Du, I. Skachko, F. Duerr, A. Luican, and E. Y. Andrei, *Fractional quantum Hall effect and insulating phase of Dirac electrons in graphene*, Nature **462**, 192 (2009).

[13] K. I. Bolotin, F. Ghahari, M. D. Shulman, H. L. Stormer, and P. Kim, *Observation of the fractional quantum Hall effect in graphene*, Nature **462**, 196 (2009).

[14] B. A. Piot, J. Kunc, M. Potemski, D. K. Maude, C. Betthausen, A. Vogl, D. Weiss, G. Karczewski, and T. Wojtowicz, *Fractional quantum Hall effect in CdTe*, Phys. Rev. B **82**, 081307(R) (2010).

[15] A. Tsukazaki, S. Akasaka, K. Nakahara, Y. Ohno, H. Ohno, D. Maryenko, A. Ohtomo, and M. Kawasaki, *Observation of the fractional quantum Hall effect in an oxide*, Nature Mat. **9**, 889 (2010).

[16] Q. Shi, M. A. Zudov, C. Morrison, and M. Myronov, *Spinless composite fermions in an ultrahigh-quality strained Ge quantum well*, Phys. Rev. B **91**, 241303(R) (2015).

[17] M. K. Ma, M. S. Hossain, K. A. Villegas Rosales, H. Deng, T. Tschirky, W. Wegscheider, and M. Shayegan, *Observation of fractional quantum Hall effect in an InAs quantum well*, Phys. Rev. B **96**, 241301(R) (2017).

[18] Apart from QHSs in GaAs, electron nematic states were identified in $Sr_3Ru_2O_7$ [70], high-T_C superconductors [71, 72], URu_2Si_2 [73], WSe_2/WS_2 [74], and twisted bilayer graphene [75].

[19] Considering thermal and quantum fluctuations, several electron liquid crystal-like phases have also been proposed [76].

[20] D. V. Fil, *Piezoelectric mechanism for the orientation of stripe structures in two-dimensional electron systems*, Low Temp. Phys. **26**, 581 (2000).

[21] S. P. Koduvayur, Y. Lyanda-Geller, S. Khlebnikov, G. Csáthy, M. J. Manfra, L. N. Pfeiffer, K. W. West, and L. P. Rokhinson, *Effect of Strain on Stripe Phases in the Quantum Hall Regime*, Phys. Rev. Lett. **106**, 016804 (2011).

[22] I. Sodemann and A. H. MacDonald, *Theory of Native Orientational Pinning in Quantum Hall Nematics*, arXiv:1307.5489 [cond-mat.str-el] (2013).

[23] J. Pollanen, K. B. Cooper, S. Brandsen, J. P. Eisenstein, L. N. Pfeiffer, and K. W. West, *Heterostructure symmetry and the orientation of the quantum Hall nematic phases*, Phys. Rev. B **92**, 115410 (2015).

[24] QHSs were found to align along $\langle 1\bar{1}0 \rangle$ direction in a tunable density heterostructure insulated gate field effect transistor at densities n_e between 3×10^{11} cm^{-2} and 4.6×10^{11} cm^{-2} [77] and in single heterointerface devices with $n_e \simeq 2 \times 10^{11}$ cm^{-2} and cap thickness exceeding 1 μm [23].

[25] Indeed, anisotropies emerging under in-plane magnetic field, which is known to provide symmetry breaking [78–84], have been observed in ZnO [85] and AlAs [86].

[26] K. B. Cooper, M. P. Lilly, J. P. Eisenstein, L. N. Pfeiffer, and K. W. West, *Insulating phases of two-dimensional electrons in high Landau levels: Observation of sharp thresholds to conduction*, Phys. Rev. B **60**, R11285 (1999).

[27] J. P. Eisenstein, K. B. Cooper, L. N. Pfeiffer, and K. W. West, *Insulating and Fractional Quantum Hall States in the First Excited Landau Level*, Phys. Rev. Lett. **88**, 076801 (2002).

[28] R. M. Lewis, P. D. Ye, L. W. Engel, D. C. Tsui, L. N. Pfeiffer, and K. W. West, *Microwave Resonance of the Bubble Phases in 1/4 and 3/4 Filled High Landau Levels*, Phys. Rev. Lett. **89**, 136804 (2002).

[29] N. Deng, A. Kumar, M. J. Manfra, L. N. Pfeiffer, K. W. West, and G. A. Csáthy, *Collective Nature of the Reentrant Integer Quantum Hall States in the Second Landau Level*, Phys. Rev. Lett. **108**, 086803 (2012).

[30] A. V. Rossokhaty, Y. Baum, J. A. Folk, J. D. Watson, G. C. Gardner, and M. J. Manfra, *Electron-Hole Asymmetric Chiral Breakdown of Reentrant Quantum Hall States*, Phys. Rev. Lett. **117**, 166805 (2016).

[31] B. Friess, Y. Peng, B. Rosenow, F. von Oppen, V. Umansky, K. von Klitzing, and J. H. Smet, *Negative permittivity in bubble and stripe phases*, Nature Phys. **13**, 1124 (2017).

[32] K. Bennaceur, C. Lupien, B. Reulet, G. Gervais, L. N. Pfeiffer, and K. W. West, *Competing Charge Density Waves Probed by Nonlinear Transport and Noise in the Second and Third Landau Levels*, Phys. Rev. Lett. **120**, 136801 (2018).

[33] B. Friess, V. Umansky, K. von Klitzing, and J. H. Smet, *Current Flow in the Bubble and Stripe Phases*, Phys. Rev. Lett. **120**, 137603 (2018).

[34] X. Fu, Q. Shi, M. A. Zudov, G. C. Gardner, J. D. Watson, and M. J. Manfra, *Two- and three-electron bubbles in* $Al_xGa_{1-x}As/Al_{0.24}Ga_{0.76}As$ *quantum wells*, Phys. Rev. B **99**, 161402(R) (2019).

[35] D. Ro, N. Deng, J. D. Watson, M. J. Manfra, L. N. Pfeiffer, K. W. West, and G. A. Csáthy, *Electron bubbles and the structure of the orbital wave function*, Phys. Rev. B **99**, 201111(R) (2019).

[36] S. Chen, R. Ribeiro-Palau, K. Yang, K. Watanabe, T. Taniguchi, J. Hone, M. O. Goerbig, and C. R. Dean, *Competing Fractional Quantum Hall and Electron Solid Phases in Graphene*, Phys. Rev. Lett. **122**, 026802 (2019).

[37] Y. Huang, M. Sammon, M. A. Zudov, and B. I. Shklovskii, *Isotropically conducting (hidden) quantum Hall stripe phases in a two-dimensional electron gas*, Phys. Rev. B **101**, 161302(R) (2020).

[38] A. H. MacDonald and M. P. A. Fisher, *Quantum theory of quantum Hall smectics*, Phys. Rev. B **61**, 5724 (2000).

[39] M. Sammon, X. Fu, Y. Huang, M. A. Zudov, B. I. Shklovskii, G. C. Gardner, J. D. Watson, M. J. Manfra, K. W. Baldwin, L. N. Pfeiffer, et al., *Resistivity anisotropy of quantum Hall stripe phases*, Phys. Rev. B **100**, 241303(R) (2019).

[40] The mean free path along stripes limited by isotropic impurity scattering can be calculated using $L_y^2 =$

$(1/2\pi)\int_0^{2\pi} d\theta(2R_c\cos\theta)^2 = 2R_c^2$.

[41] T. Ando and Y. Uemura, *Theory of Quantum Transport in a Two-Dimensional Electron System under Magnetic Fields. I. Characteristics of Level Broadening and Transport under Strong Fields*, J. Phys. Soc. Jpn. **36**, 959 (1974).

[42] P. T. Coleridge, P. Zawadzki, and A. S. Sachrajda, *Peak values of resistivity in high-mobility quantum-Hall-effect samples*, Phys. Rev. B **49**, 10798 (1994).

[43] Our estimates show that $\Delta\nu$ reaches a maximum of 6 at $x \approx 0.1\,\%$.

[44] G. C. Gardner, J. D. Watson, S. Mondal, N. Deng, G. A. Csáthy, and M. J. Manfra, *Growth and electrical characterization of $Al_{0.24}Ga_{0.76}As/Al_xGa_{1-x}As/\ Al_{0.24}Ga_{0.76}As$ modulation-doped quantum wells with extremely low x*, Appl. Phys. Lett. **102**, 252103 (2013).

[45] In general, α should be modified by a factor $\sqrt{2\gamma}$, where γ is a parameter depending on the nature of scattering [39]. In samples without alloy disorder, γ decreases with N_1/N_2 where N_1 (N_2) is the concentration of Coulomb impurities in the barrier (quantum well), starting from $\gamma \approx 0.43$ at $N_1 = N_2$ [39], whereas in samples where scattering is dominated by alloy disorder $\gamma \approx 0.53$ [37]. While we estimate $\gamma \approx 0.4$ in our samples A and B, we will assume $\gamma = 0.5$ for simplicity.

[46] Q. Shi, *Magnetotransport in quantum Hall systems at high Landau levels*, Ph.D. thesis, University of Minnesota (2017).

[47] M. E. Raikh and T. V. Shahbazyan, *High Landau levels in a smooth random potential for two-dimensional electrons*, Phys. Rev. B **47**, 1522 (1993).

[48] A. D. Mirlin, E. Altshuler, and P. Wölfle, *Quasiclassical approach to impurity effect on magnetooscillations in 2D metals*, Ann. Phys. **508**, 281 (1996).

[49] Q. Shi, S. A. Studenikin, M. A. Zudov, K. W. Baldwin, L. N. Pfeiffer, and K. W. West, *Microwave photoresistance in an ultra-high-quality GaAs quantum well*, Phys. Rev. B **93**, 121305(R) (2016).

[50] Q. Shi, M. A. Zudov, I. A. Dmitriev, K. W. Baldwin, L. N. Pfeiffer, and K. W. West, *Fine structure of high-power microwave-induced resistance oscillations*, Phys. Rev. B **95**, 041403(R) (2017).

[51] M. A. Zudov, I. A. Dmitriev, B. Friess, Q. Shi, V. Umansky, K. von Klitzing, and J. Smet, *Hall field-induced resistance oscillations in a tunable-density GaAs quantum well*, Phys. Rev. B **96**, 121301(R) (2017).

[52] M. A. Zudov, R. R. Du, J. A. Simmons, and J. L. Reno, *Shubnikov–de Haas-like oscillations in millimeterwave photoconductivity in a high-mobility two-dimensional electron gas*, Phys. Rev. B **64**, 201311(R) (2001).

[53] P. D. Ye, L. W. Engel, D. C. Tsui, J. A. Simmons, J. R. Wendt, G. A. Vawter, and J. L. Reno, *Giant microwave photoresistance of two-dimensional electron gas*, Appl. Phys. Lett. **79**, 2193 (2001).

[54] I. A. Dmitriev, A. D. Mirlin, D. G. Polyakov, and M. A. Zudov, *Nonequilibrium phenomena in high Landau levels*, Rev. Mod. Phys. **84**, 1709 (2012).

[55] C. L. Yang, J. Zhang, R. R. Du, J. A. Simmons, and J. L. Reno, *Zener Tunneling Between Landau Orbits in a High-Mobility Two-Dimensional Electron Gas*, Phys. Rev. Lett. **89**, 076801 (2002).

[56] W. Zhang, H.-S. Chiang, M. A. Zudov, L. N. Pfeiffer, and K. W. West, *Magnetotransport in a two-dimensional electron system in dc electric fields*, Phys. Rev. B **75**, 041304(R) (2007).

[57] M. G. Vavilov, I. L. Aleiner, and L. I. Glazman, *Nonlinear resistivity of a two-dimensional electron gas in a magnetic field*, Phys. Rev. B **76**, 115331 (2007).

[58] P. Coleridge, M. Hayne, P. Zawadzki, and A. Sachrajda, *Effective masses in high-mobility 2D electron gas structures*, Surf. Sci. **361**, 560 (1996).

[59] Y.-W. Tan, J. Zhu, H. L. Stormer, L. N. Pfeiffer, K. W. Baldwin, and K. W. West, *Measurements of the Density-Dependent Many-Body Electron Mass in Two Dimensional GaAs/AlGaAs Heterostructures*, Phys. Rev. Lett. **94**, 016405 (2005).

[60] A. T. Hatke, M. A. Zudov, J. D. Watson, M. J. Manfra, L. N. Pfeiffer, and K. W. West, *Evidence for effective mass reduction in GaAs/AlGaAs quantum wells*, Phys. Rev. B **87**, 161307(R) (2013).

[61] A. V. Shchepetilnikov, D. D. Frolov, Y. A. Nefyodov, I. V. Kukushkin, and S. Schmult, *Renormalization of the effective mass deduced from the period of microwave-induced resistance oscillations in GaAs/AlGaAs heterostructures*, Phys. Rev. B **95**, 161305(R) (2017).

[62] X. Fu, Q. A. Ebner, Q. Shi, M. A. Zudov, Q. Qian, J. D. Watson, and M. J. Manfra, *Microwave-induced resistance oscillations in a back-gated GaAs quantum well*, Phys. Rev. B **95**, 235415 (2017).

[63] The resistivities represented by ▲, △ (▼, ▽) were obtained from R_{xx} and R_{yy} [87] (R_{xx} and theoretical resistivity product [38]), see Ref. 39 for details.

[64] The analysis of the anisotropy ratio in this sample [39] with theoretical value of $\alpha = 18$ leads to $\gamma \approx 0.15$ (see also Ref. 45) and a ratio of concentrations of Coulomb impurities in the spacer N_1 to that in the quantum well N_2, $N_1/N_2 \simeq 60$, much larger than $N_1/N_2 \simeq 10$ estimated in Ref. 88. Our present experiments, however, suggest lower value of α, leading to larger γ and restoring the agreement with Ref. 88. Larger γ can also result from interface roughness scattering which was not theoretically considered in Ref. 88.

[65] Q. Qian, J. Nakamura, S. Fallahi, G. C. Gardner, and M. J. Manfra, *Possible nematic to smectic phase transition in a two-dimensional electron gas at half-filling*, Nature Commun. **8**, 1536 (2017).

[66] X. Fu, Q. Shi, M. A. Zudov, G. C. Gardner, J. D. Watson, M. J. Manfra, K. W. Baldwin, L. N. Pfeiffer, and K. W. West, *Anomalous Nematic States in High Half-filled Landau Levels*, Phys. Rev. Lett. **124**, 067601 (2020).

[67] With $i, j = x, y$ ($i \neq j$), the resistivity in units of h/e^2 is $\tilde{\rho}_{ii} \simeq \tilde{\sigma}_{jj}\nu^{-2}$, where $\tilde{\sigma}_{jj} = L_j/2L_i$ and L_i (L_j) is the mean free path along i (j) direction. Without dislocations, $L_y \propto \nu^{-1}$, $L_x \propto \nu$ and $\tilde{\rho}_{xx} \propto \nu^{-4}$ while $\tilde{\rho}_{yy} \propto \nu^0$. With dislocations, $L_y \propto L_x \propto \nu$, i.e., $\tilde{\sigma}_{jj} \propto \nu^0$, and $\tilde{\rho}_{xx} \propto \tilde{\rho}_{yy} \propto \nu^{-2}$.

[68] Eqs (7) and (8) can be obtained via replacement of hopping time of electrons between neighboring stripes $2\tau_B$ by L_d/v, where v is the drift velocity of electron along the stripe.

[69] The approximate condition for the hQHS phase detection is $\tilde{\sigma}_0 > \alpha^2(\tau/\tau_\mathrm{q})\max\{\tau/\tau_\mathrm{q}, 11/2\}$.

[70] R. A. Borzi, S. A. Grigera, J. Farrell, R. S. Perry, S. J. S. Lister, S. L. Lee, D. A. Tennant, Y. Maeno, and A. P. Mackenzie, *Formation of a Nematic Fluid at High Fields in $Sr_3Ru_2O_7$*, Science **315**, 214 (2007).

[71] R. Daou, J. Chang, D. LeBoeuf, O. Cyr-Choiniere, F. Laliberte, N. Doiron-Leyraud, B. J. Ramshaw, R. Liang, D. A. Bonn, W. N. Hardy, et al., *Broken rotational symmetry in the pseudogap phase of a high-Tc superconductor*, Nature **463**, 519 (2010).

[72] J.-H. Chu, J. G. Analytis, K. De Greve, P. L. McMahon, Z. Islam, Y. Yamamoto, and I. R. Fisher, *In-Plane Resistivity Anisotropy in an Underdoped Iron Arsenide Superconductor*, Science **329**, 824 (2010).

[73] R. Okazaki, T. Shibauchi, H. J. Shi, Y. Haga, T. D. Matsuda,

E. Yamamoto, Y. Onuki, H. Ikeda, and Y. Matsuda, *Rotational Symmetry Breaking in the Hidden-Order Phase of URu_2Si_2*, Science **331**, 439 (2011).

[74] C. Jin, Z. Tao, T. Li, Y. Xu, Y. Tang, J. Zhu, S. Liu, K. Watanabe, T. Taniguchi, J. C. Hone, et al., *Stripe phases in WSe_2/WS_2 moiré superlattices*, arXiv:2007.12068 (2020).

[75] Y. Cao, D. Rodan-Legrain, J. M. Park, F. N. Yuan, K. Watanabe, T. Taniguchi, R. M. Fernandes, L. Fu, and P. Jarillo-Herrero, *Nematicity and Competing Orders in Superconducting Magic-Angle Graphene*, arXiv:2004.04148 (2020).

[76] E. Fradkin and S. A. Kivelson, *Liquid-crystal phases of quantum Hall systems*, Phys. Rev. B **59**, 8065 (1999).

[77] J. Zhu, W. Pan, H. L. Stormer, L. N. Pfeiffer, and K. W. West, *Density-Induced Interchange of Anisotropy Axes at Half-Filled High Landau Levels*, Phys. Rev. Lett. **88**, 116803 (2002).

[78] W. Pan, R. R. Du, H. L. Stormer, D. C. Tsui, L. N. Pfeiffer, K. W. Baldwin, and K. W. West, *Strongly Anisotropic Electronic Transport at Landau Level Filling Factor under a Tilted Magnetic Field*, Phys. Rev. Lett. **83**, 820 (1999).

[79] M. P. Lilly, K. B. Cooper, J. P. Eisenstein, L. N. Pfeiffer, and K. W. West, *Anisotropic States of Two-Dimensional Electron Systems in High Landau Levels: Effect of an In-Plane Magnetic Field*, Phys. Rev. Lett. **83**, 824 (1999).

[80] T. Jungwirth, A. H. MacDonald, L. Smrčka, and S. M. Girvin, *Field-tilt anisotropy energy in quantum Hall stripe states*, Phys. Rev. B **60**, 15574 (1999).

[81] T. D. Stanescu, I. Martin, and P. Phillips, *Finite-Temperature Density Instability at High Landau Level Occupancy*, Phys. Rev. Lett. **84**, 1288 (2000).

[82] H. Zhu, G. Sambandamurthy, L. W. Engel, D. C. Tsui, L. N. Pfeiffer, and K. W. West, *Pinning Mode Resonances of 2D Electron Stripe Phases: Effect of an In-Plane Magnetic Field*, Phys. Rev. Lett. **102**, 136804 (2009).

[83] Q. Shi, M. A. Zudov, J. D. Watson, G. C. Gardner, and M. J. Manfra, *Evidence for a new symmetry breaking mechanism reorienting quantum Hall nematics*, Phys. Rev. B **93**, 121411(R) (2016).

[84] Q. Shi, M. A. Zudov, Q. Qian, J. D. Watson, and M. J. Manfra, *Effect of density on quantum Hall stripe orientation in tilted magnetic fields*, Phys. Rev. B **95**, 161303(R) (2017).

[85] J. Falson, D. Tabrea, D. Zhang, I. Sodemann, Y. Kozuka, A. Tsukazaki, M. Kawasaki, K. von Klitzing, and J. H. Smet, *A cascade of phase transitions in an orbitally mixed half-filled Landau level*, Science Advances **4** (2018), http://advances.sciencemag.org/content/4/9/eaat8742.full.pdf.

[86] M. S. Hossain, M. A. Mueed, M. K. Ma, Y. J. Chung, L. N. Pfeiffer, K. W. West, K. W. Baldwin, and M. Shayegan, *Anomalous coupling between magnetic and nematic orders in quantum Hall systems*, Phys. Rev. B **98**, 081109(R) (2018).

[87] S. H. Simon, *Comment on "Evidence for an Anisotropic State of Two-Dimensional Electrons in High Landau Levels"*, Phys. Rev. Lett. **83**, 4223 (1999).

[88] M. Sammon, M. A. Zudov, and B. I. Shklovskii, *Mobility and quantum mobility of modern GaAs/AlGaAs heterostructures*, Phys. Rev. Materials **2**, 064604 (2018).